Investigation of the dynamic Stark effect in a $J=0\rightarrow1\rightarrow0$ three-level system. III. The "strong-probe" case

P. T. H. Fisk, H.-A. Bachor, and R. J. Sandeman
Department of Physics and Theoretical Physics, The Australian National University, Canberra 2601, Australia
(Received 4 August 1986)

We have investigated the dynamic Stark effect in a $J=0\rightarrow1\rightarrow0$ three-level ladder system in an atomic beam of natural barium. An intense, actively stabilized cw dye laser was tuned to resonance between the upper two levels, and a similar laser was scanned through resonance with the transition connecting the lower two levels. Fluorescence arising from transitions out of the middle and upper levels was separately recorded as a function of probe laser frequency. This is the third and final paper in a series, of which the first two papers investigated theoretically and experimentally the "weak-probe" case, where the intensity of the probe laser was sufficiently low for the interaction between the atoms and the probe laser to be linear. In this paper we present an experimental investigation of the "strong-probe" case, where both lasers interact nonlinearly with the atoms, and we compare the results with the predictions of a theoretical model based on the optical Bloch equations.

I. INTRODUCTION

In recent years there have been several investigations of the dynamic Stark effect in Doppler-free (atomic beam) optical double-resonance experiments.[1–4] Most of these experiments used three-level systems (3LS's) in an atomic beam of sodium. A strong perturbing laser was tuned to resonance between the ground state and middle level of the 3LS, and a weak probe laser was scanned through resonance with the transition connecting the middle and upper levels. Fluorescence from the upper level was monitored as a function of probe-laser frequency. This generally resulted in a two-peaked profile, known as an Autler-Townes doublet, which is symmetrical when the strong laser is tuned to exact resonance, and becomes asymmetrical as the strong laser is detuned. With the strong laser tuned to exact resonance, the separation (in angular frequency units) of the two peaks is equal to the Rabi frequency $\beta=\boldsymbol{\mu}\cdot\mathbf{E}/\hbar$, where $\boldsymbol{\mu}$ is the dipole moment of the transition driven by the strong laser, $|\mathbf{E}|$ is the electric field amplitude of the laser light, and $\hbar$ is Planck's constant divided by 2π.

More recently, we have investigated experimentally[5] and theoretically[6] the case where the strong laser was tuned to the transition connecting the upper two levels of a 3LS in barium, and the weak-probe laser was scanned through resonance with the transition connecting the lower two levels. Fluorescence from the middle and upper levels was independently monitored as a function of probe-laser frequency for a range of strong-laser detunings. The results of this "weak-probe" investigation were in excellent agreement with theory.

As an extension to this work,[5,6] we present in this paper the results and comparison with theory of an almost identical experiment, but where the intensity of the "probe"[7] laser was increased so that it also interacted nonlinearly with the atoms. This type of situation arises in many experiments involving multistep laser excitation of atoms or molecules, but few systematic experimental investigations have been published.[3]

II. EXPERIMENT

The atomic system in ^{138}Ba,[8–10] shown in Fig. 1, and the experimental arrangement and method used for the present (strong-probe) experiment are identical to that

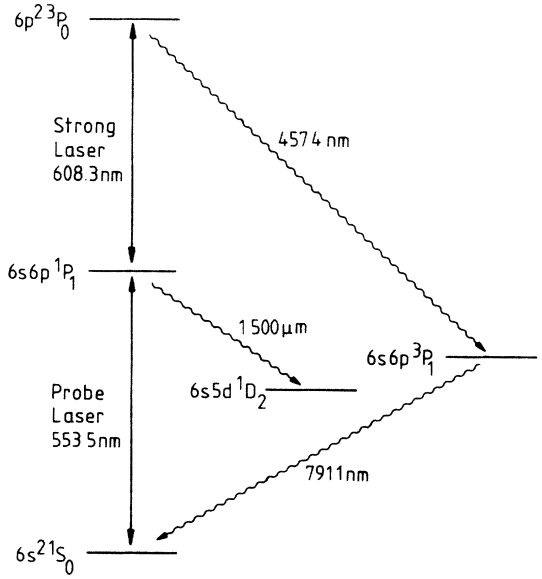

FIG. 1. System of atomic levels in ^{138}Ba involved in the experiment. Relevant atomic parameters are oscillator strengths (f): $6s^2\,{}^1S_0\rightarrow6s6p\,{}^1P_1$, $f=1.64$ (Ref. 8), $6s6p\,{}^1P_1\rightarrow6p^2\,{}^3P_0$, $f=0.0078$ (Ref. 5). Lifetimes (τ): $6s6p\,{}^1P_1$, $\tau=8.4$ ns (Ref. 9), $6p^2\,{}^3P_0$, $\tau=6.2$ ns (Ref. 10). The $6s5d\,{}^1D_2$ level is metastable. Branching ratios (r): $6p^2\,{}^3P_0\rightarrow6s6p\,{}^1P_1$, $r=2.6\%$ (Ref. 5), $6s6p\,{}^1P_1\rightarrow6s^2\,{}^1S_0$, $r\geq98.5\%$ (Ref. 8).

used in the weak-probe experiment, and are described in detail elsewhere.[5,6] Briefly, a laser tuned to 608.3 nm (the strong laser) and a laser tuned to 553.5 nm (the probe laser), were focused onto an atomic beam of natural barium. The frequency jitter of the two lasers and the residual Doppler width of the atomic beam were small compared with the natural linewidths of the transitions being driven. The intensity of the 553.5- and 457.4-nm fluorescence, resulting from transitions from the middle ($6s6p\ ^1P_1$) and upper ($6p^2\ ^3P_0$) levels, respectively, was independently recorded as the 553.5-nm probe laser was scanned. The dependence of the resulting profiles on the detuning and intensity of the strong laser, and on the intensity of the probe laser, was investigated.

In the present (strong-probe) work, the intensity of the probe beam was varied (using neutral density filters) over the range 22 W/m^2–2.7 kW/m^2, corresponding to probe-laser Rabi frequencies of 9–100 MHz. For comparison, the probe-laser intensity in the weak-probe experiment[5] was 2.4 W/m^2, corresponding to a Rabi frequency of 3 MHz.

III. RESULTS

A series of profiles obtained with different probe-laser Rabi frequencies, and with the strong laser tuned to resonance (± 3 MHz), is shown in Fig. 2. Throughout this paper, a positive detuning indicates that the frequency of the laser light is greater than that of the atomic transition being driven. The profiles are all normalized to the same peak amplitude. In the weak-probe case (probe-laser Rabi frequency 3 MHz), the profiles of both the middle and upper levels exhibit the well-known Autler-Townes doublet.[1–5] The primary effect on these profiles of increasing the probe-laser intensity is that of power broadening. For this particular strong-laser Rabi frequency (200 ± 5 MHz), the Autler-Townes doublet is no longer resolved in either the middle- or upper-level profiles when the probe-laser Rabi frequency is greater than 95 MHz.

The asymmetry of the Autler-Townes doublets is due to isotopes of barium other than ^{138}Ba.[5,6] These other isotopes are also responsible for the smaller peaks to the right (larger probe-laser detuning) of the Autler-Townes doublets in both the middle and upper-level profiles.

Figure 3 shows a series of profiles obtained with the same experimental parameters as for the profiles shown in Fig. 2, except that the strong laser was detuned from resonance by -400 ± 10 MHz. As was previously observed in the weak-probe case,[5] the upper-level profiles consist of two main peaks, one close to the unperturbed resonance position (zero probe-laser detuning) and the other close to the two-photon resonance (where the sum of the strong-laser and probe-laser detunings is zero). The middle-level profiles consist of only one peak, the peak near the two-photon resonance being suppressed by the same process responsible for coherent population trapping.[11,12,5] The numerous smaller peaks in both the upper- and middle-level profiles are again due to isotopes other than ^{138}Ba.

The most interesting feature of the profiles shown in Fig. 3 is that as the intensity of the probe laser is increased, the profiles are not only power broadened, but the relative heights of the two peaks of the Autler-Townes doublet are gradually reversed. Such behavior is significant for two-step excitation experiments which aim to maximize the population of the uppermost level.

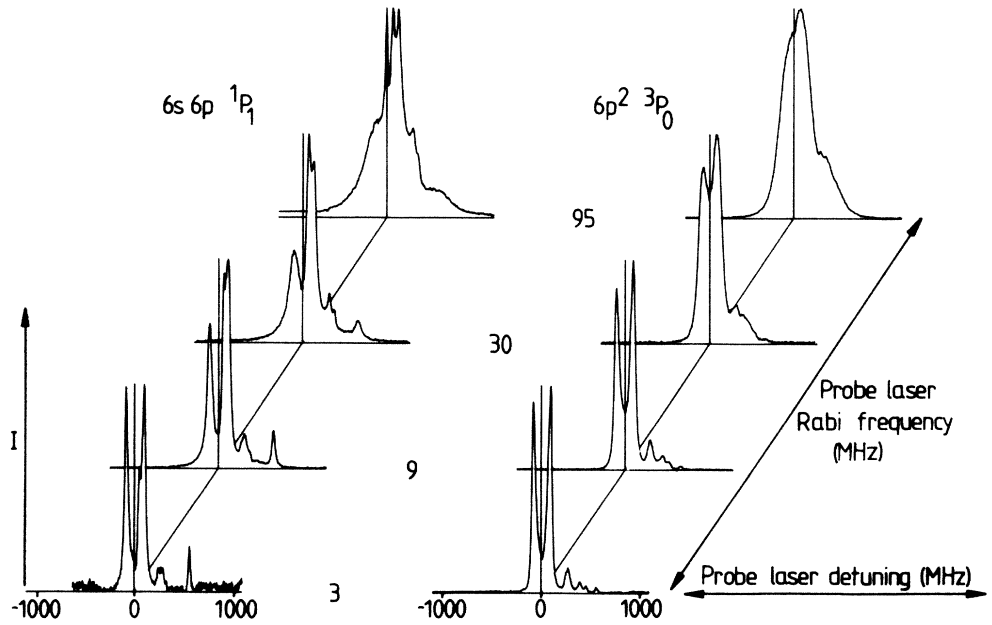

FIG. 2. Comparison of experimental results obtained with four different probe-laser Rabi frequencies. The strong-laser Rabi frequency was 200 ± 5 MHz, and the strong laser was tuned to line center. For each probe-laser Rabi frequency, the intensity of fluorescence I is plotted against the detuning of the probe laser from line center. The $6s6p\ ^1P_1$ and $6p^2\ ^3P_0$ profiles represent the intensity of the 553.5- and 457.4-nm fluorescence, respectively.

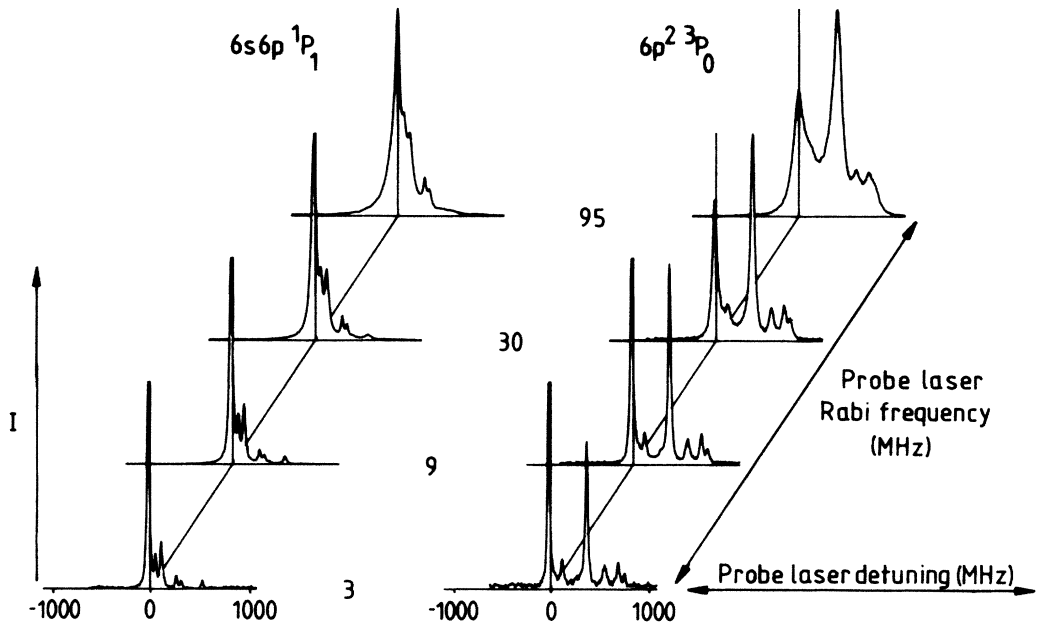

FIG. 3. Comparison of experimental results obtained with four different probe-laser Rabi frequencies. The strong-laser Rabi frequency was 200±5 MHz, and the strong laser was detuned −400±10 MHz from line center.

Figure 4 demonstrates the dependence of the profiles on the detuning of the strong laser. In this figure the intensity scales for middle- and upper-level profiles are unrelated.

It is interesting to compare Fig. 4 with Fig. 3 of our earlier work,[5] which shows a corresponding series of profiles obtained in the weak-probe regime. This comparison shows that the dependence of the middle-level profiles on the strong-laser detuning is similar in both the weak- and strong-probe regimes. In the case of the upper-level profiles, the peak amplitude of the component of the Autler-Townes doublet which remains closest to the unperturbed resonance (zero probe-laser detuning) as the strong laser is detuned shows a similar dependence on the strong-laser

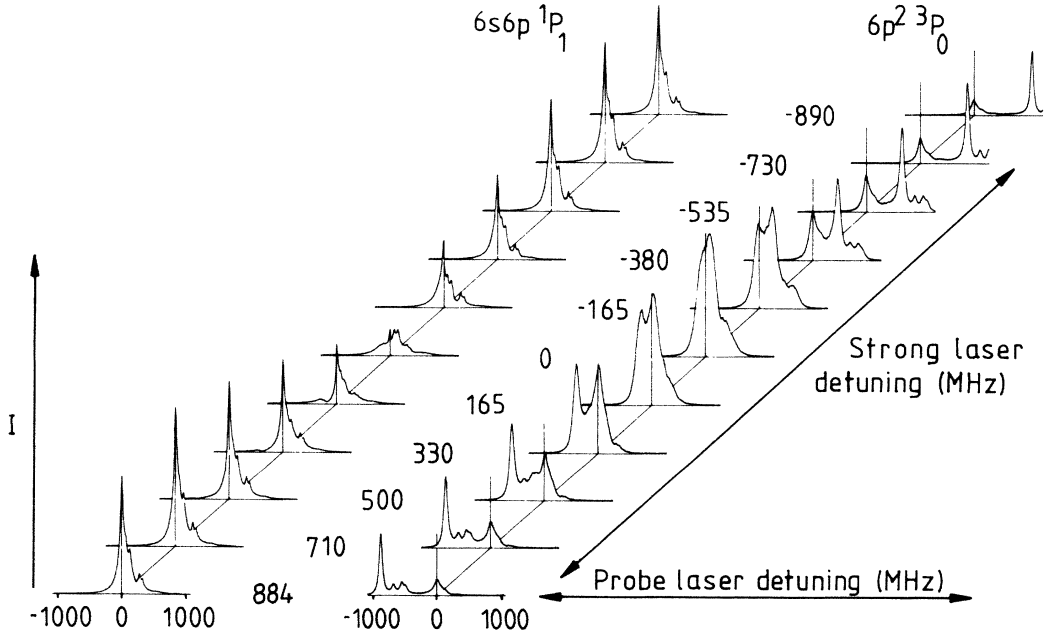

FIG. 4. Experimental profiles obtained with a strong-laser Rabi frequency of 200±5 MHz and a probe-laser Rabi frequency of 95±5 MHz.

detuning in both the weak- and strong-probe regimes. The strong-laser detuning dependence of the component at the two-photon resonance, however, is markedly different in the two regimes. It therefore appears that apart from power broadening of the profiles, the most significant effect, on the shape of the profiles, of increasing the probe-laser intensity from the linear regime to the nonlinear regime in this particular atomic system is to increase the amplitude of the component of the Autler-Townes doublet at the two-photon resonance in the upper-level fluorescence.

IV. THEORETICAL DESCRIPTION

The theoretical description of the nonlinear interaction between the system of laser radiation fields and atomic energy levels shown in Fig. 1 is considerably more involved in the strong-probe case than in the weak-probe case.[6] In the weak-probe case it was reasonable to assume that the detectors predominantly recorded the steady-state response of the atoms. It was also possible to restrict the theoretical model to a system of three levels ($6s^2\,^1S_0 \rightarrow 6s\,6p\,^1P_1 \rightarrow 6p^2\,^3P_0$) with a generalized relaxation path out of the 3LS from the upper ($6p^2\,^3P_0$) level.[6] Thus it was not necessary to include in the theoretical model all external levels to which the upper level relaxes. Both these assumptions were justified by noting that in the weak-probe case the population of the ground state is not significantly disturbed by the lasers. Therefore, during the transit time (600 ns) of the atoms across the laser beams, the proportion of the total population pumped into levels external to the 3LS will be negligible and any atom relaxing back to the ground state is unlikely to make any further contribution to the observed signals.

In the strong-probe case, neither of the above assumptions is valid, since it is possible for a significant proportion of the ground-state population to be pumped into the long-lived $6s\,6p\,^3P_1$ and $6s\,5d\,^1D_2$ levels, which do not interact with the laser radiation. Thus the fluorescence observed by the detectors is likely to be a transient response of the atoms before they are pumped into the long-lived levels external to the 3LS. It was therefore necessary to include all the atomic levels shown in Fig. 1 in the theoretical model.

The contribution of ^{138}Ba to the results of the present experiment was therefore modeled by treating the atomic beam passing through the two collinear, counterpropagating laser beams as an ensemble of stationary atoms subjected to two simultaneous pulses of laser light (one of 553.5 nm, the other of 608.3 nm), with Gaussian intensity profiles in the time domain. The widths of these pulses were equal to the average transit time of the atoms across the corresponding laser beams. The probe-laser pulse was shorter than the strong-laser pulse because the probe laser was focused more tightly than the strong laser at the interaction region, where the laser beams crossed the atomic beam. For each combination of laser intensities and detunings used in the experimental profiles, the optical Bloch equations[13] were solved numerically[14] to obtain the time development of the populations of the five atomic levels shown in Fig. 1, as the atoms in the atomic beam passed through the laser beams. The observed signals are proportional to the time-integrated populations of the $6s\,6p\,^1P_1$ and $6p^2\,^3P_0$ levels, and the theoretical profiles were obtained by repeating this calculation for a continuous range of probe-laser detunings.

Although approximately 11% (Ref. 15) of the population of the $6p^2\,^3P_0$ level relaxes to the $5d\,6p\,^3D_1$ level (not shown on Fig. 1), it was found that the effects of this relaxation path on the profiles generated by the theoretical model were negligible compared with the effects of relaxation from the $6p^2\,^3P_0$ level to the $6s\,6p\,^3P_1$ level. Therefore, in order to simplify the theoretical model, it was assumed that the population of the $6p^2\,^3P_0$ level relaxes only to the $6s\,6p\,^1P_1$ and $6s\,6p\,^3P_1$ levels.

Figure 5 shows an example of the time dependence of the diagonal density-matrix elements (populations) of the three levels of the 3LS (χ_{00}, χ_{11}, χ_{22}) and the total population of the levels ($6s\,6p\,^3P_1$ and $6s\,5d\,^1D_2$) external to the 3LS (χ_{33}), for parameters corresponding to the peak of the upper-level profile obtained with a probe-laser Rabi frequency of 95 MHz shown in Fig. 2. This figure confirms that in the strong-probe regime, the observed signals are due to a transient response, since the ground-state population is almost entirely depleted before the atoms reach the center of the laser beams. Thus for this combination of laser intensities and detunings, the effective Rabi frequencies of the strong and probe lasers are somewhat smaller than would be calculated from their peak intensities. It is therefore clear that for this atomic system, to neglect the effect of long-lived levels external to the 3LS in the strong-probe regime would lead to profiles which would not be in agreement with the experimental results.

In order to compare the experimental and theoretical profiles in detail, it is necessary to take full account of the Gaussian intensity profiles of the laser beams, and the isotope structure of barium. The above technique automatically takes into account the Gaussian intensity profiles of the laser beams as measured along the axis of the atomic beam, and the populations plotted in Fig. 7 correspond to atoms in the atomic beam whose paths take them through the center of the laser beams. However, the diameter of the atomic beam was not small compared with the diameters of the laser beams,[5] so that there is a significant contribution from atoms which pass through the edges of the circularly symmetric laser intensity profiles, and thus see shorter, less intense light pulses. To account for this, the atomic beam was divided into 20 slices parallel to its axis. The contributions to the total signal from the atoms in each slice, which see laser pulses of different intensities and durations, were calculated separately and then added.[14]

The isotopic composition of natural barium is (in atomic percent) 71.9% ^{138}Ba, 11.2% ^{137}Ba, 7.8% ^{136}Ba, 6.5% ^{135}Ba, and 2.4% ^{134}Ba. All of these isotopes contribute significantly to the observed profiles. The contribution due to the isotopes of barium other than ^{138}Ba were included in the theoretical model using the same method as was used in the modeling of the weak-probe experiment. This method, which is described in detail elsewhere,[6] involved evaluating the time-integrated level populations of

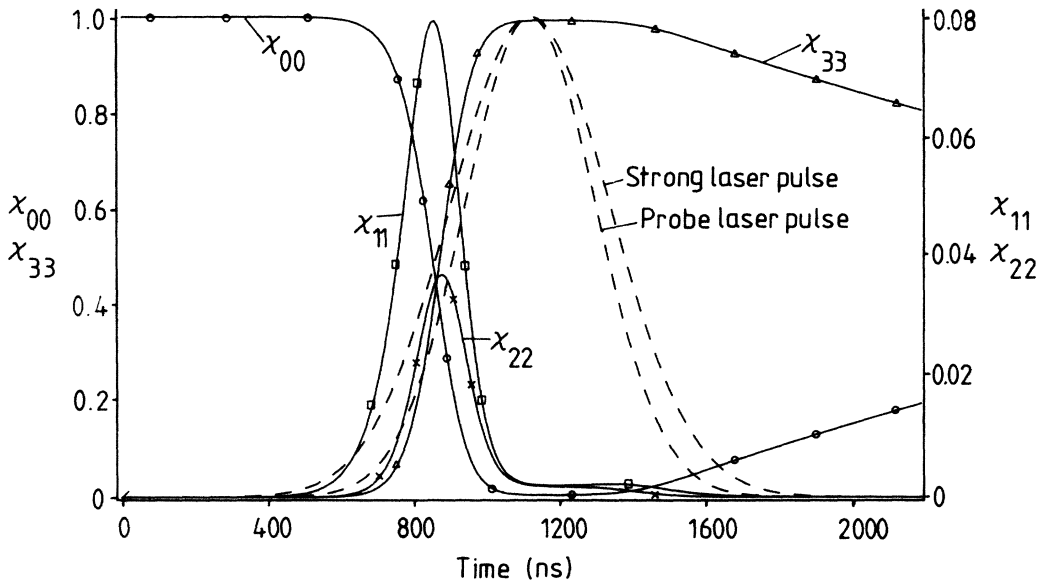

FIG. 5. Calculated time evolution of the diagonal density-matrix elements (populations) χ for the system of atomic levels shown in Fig. 1. The strong- and probe-laser pulses were assumed to be Gaussian with full width at half maximums (FWHM) of 423 and 347 ns, respectively, corresponding to the average time of flight of the atoms across the laser beams. The laser parameters were strong laser; Rabi frequency 200 MHz, detuning 0 MHz. Probe laser; Rabi frequency 95 MHz, detuning 100 MHz. The symbols χ_{00}, χ_{11}, and χ_{22} represent the diagonal density-matrix elements for the $6s^2\,{}^1S_0$, $6s6p\,{}^1P_1$, and $6p^2\,{}^3P_0$ levels, respectively, and χ_{33} represents the sum of the diagonal density-matrix elements for the $6s6p\,{}^3P_1$ and $6s5d\,{}^1D_2$ levels.

the five main isotopes of barium separately, weighting them according to their abundance and the geometry of the experiment, and then adding them to give the final profiles. The isotopes ^{136}Ba and ^{134}Ba have, as does ^{138}Ba, nuclear spin $I=0$, resulting in the absence of hyperfine structure in the $6s6p\,{}^1P_1$ level. Since the isotope shifts of the $6s6p\,{}^1P_1$ and $6p^2\,{}^3P_0$ levels of all the isotopes have been measured,[16,17] evaluating the contribution of these isotopes was straightforward.

Unfortunately, the isotopes ^{137}Ba and ^{135}Ba have nuclear spin $I=\frac{3}{2}$, resulting in the $6s6p\,{}^1P_1$ level having three hyperfine components, with total angular momentum quantum numbers $F=\frac{1}{2}$, $\frac{3}{2}$, and $\frac{5}{2}$. Due to the large number of Zeeman sublevels present in these isotopes (Fig. 6), the model was simplified by including only coherences between Zeeman sublevels with the same magnetic quantum number M_F, and neglecting spontaneous relaxation between Zeeman sublevels of different magnetic quantum number. Thus for the purposes of solving the Bloch equations, the 20 Zeeman sublevels comprising the $6s^2\,{}^1S_0 \rightarrow 6s6p\,{}^1P_1 \rightarrow 6p^2\,{}^3P_0$ 3LS's in ^{137}Ba and ^{135}Ba were separated into two types of Zeeman subsystems (Fig. 6), denoted by the magnetic quantum number of the sublevels involved. The contribution from each type of subsystem was evaluated by solving the Bloch equations in the same way as for the even isotopes, however, in the case of the $M_F=\frac{3}{2}$ and $M_F=\frac{1}{2}$ Zeeman subsystems the Bloch equations describe a system of six and seven levels, respectively.

In the weak-probe case, neglecting cross relaxation between the Zeeman subsystems was justified for the case of the upper-level $\rightarrow$ middle-level transition by noting that

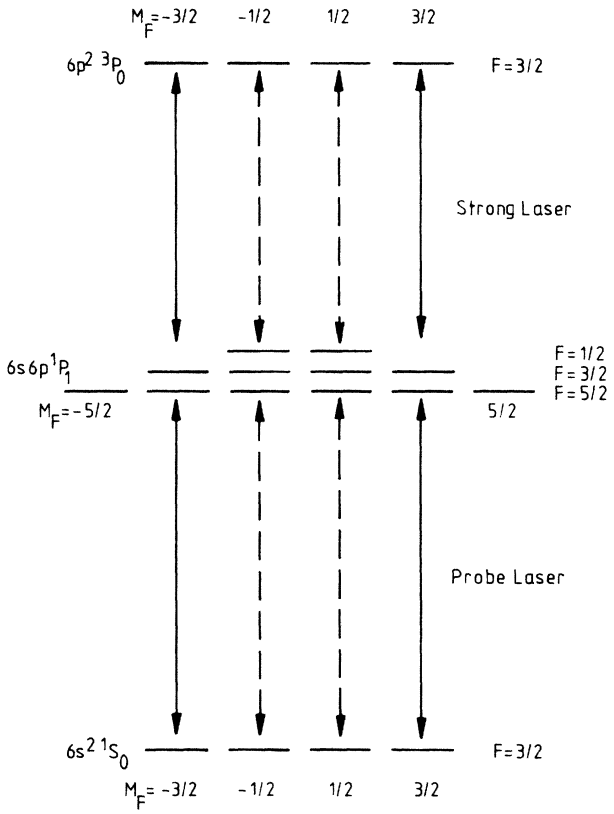

FIG. 6. Hyperfine and Zeeman structure in ^{137}Ba and ^{135}Ba. The dashed arrowed lines denote the $M_F=\frac{1}{2}$ Zeeman subsystems and the solid arrowed lines represent the $M_F=\frac{3}{2}$ Zeeman subsystems.

only 2.6% (Ref. 5) of the upper-level population relaxes to the middle level, so that only 2.6% of the atoms can be affected by such cross relaxation. For the case of the middle-level → ground-state transition, cross relaxation between the Zeeman subsystems was neglected because any atom which relaxes to the ground state via any path is unlikely to interact with the probe laser again, due to its low intensity. However, in the strong-probe case, the second of these two justifications is not valid, since as is evident from Fig. 5, the ground state is almost entirely depleted by the interaction with the laser light. Due to computer time restrictions, it was not possible to model these isotopes without the simplifications resulting from treating the Zeeman subsystems independently, due to the complexity of the Bloch equations which would otherwise have to be solved. Consequently, some disagreement between the features of the theoretical and experimental profiles due to these isotopes (which together comprise 17.7% of natural barium) is to be expected.

V. COMPARISON WITH EXPERIMENT

The experimental profiles shown in Figs. 2 and 3 are compared in Figs. 7 and 8 with theoretical profiles calculated as described in Sec. IV. The agreement between theoretical and experimental profiles is generally reasonable, with the exception of the peaks in the middle-level profiles indicated by arrows. These peaks, corresponding to the $F=\frac{1}{2}$ hyperfine components of the middle levels of ^{137}Ba and ^{135}Ba, gradually disappear in the experimental profiles as the probe-laser Rabi frequency is increased, whereas in the theoretical profiles they do not. This behavior is still evident with the strong laser blocked, as shown in Fig. 9.

The above discrepancy is one consequence of the approximation, mentioned in Sec. IV, of treating the $M_F=\frac{1}{2}$ and $M_F=\frac{3}{2}$ Zeeman subsystems in ^{137}Ba and ^{135}Ba separately. This effect is not easily understood by considering the case corresponding to Fig. 9, where the strong laser is blocked. If the probe laser is tuned to resonance with the transition connecting the ground state with the $F=\frac{1}{2}$, $M_F=\pm\frac{1}{2}$ hyperfine Zeeman sublevel of the middle level (Fig. 6), the resulting population in this sublevel will relax to the $M_F=\pm\frac{1}{2}$ and $M_F=\pm\frac{3}{2}$ Zeeman sublevels of the ground state. However, the fraction of the population which relaxes to the $M_F=\pm\frac{3}{2}$ sublevels of the ground state cannot interact further with the laser light, so that given a sufficiently long interaction time, the entire population will be pumped into these Zeeman sublevels. This optical pumping does not occur for the $F=\frac{3}{2}$ and $F=\frac{5}{2}$ components of the $M_F=\frac{1}{2}$ Zeeman subsystem or for any components of the $M_F=\frac{3}{2}$ Zeeman subsystem, so that the fluorescence peak due to the $M_F=\frac{1}{2}$ hyperfine component of the middle level will be suppressed with respect to that due to the other two components.

Since cross relaxation between the $M_F=\frac{1}{2}$ and $M_F=\frac{3}{2}$ Zeeman subsystems is excluded by the assumption that the two subsystems are independent, the optical pumping causing the suppression of the peak due to the $M_F=\frac{1}{2}$ sublevel is not predicted by the theoretical model.

This particular discrepancy could have been eliminated by a suitable adjustment of the rate of relaxation from the $F=\frac{1}{2}$, $M_F=\frac{1}{2}$ sublevel to the ground state, thus accounting for the loss of population from the $M_F=\frac{1}{2}$ Zeeman subsystem due to the relaxation of this hyperfine level. However, this technique will not account for cross relaxation occurring when the probe laser is tuned close to resonance with the $F=\frac{3}{2}$ or $F=\frac{5}{2}$ hyperfine components,

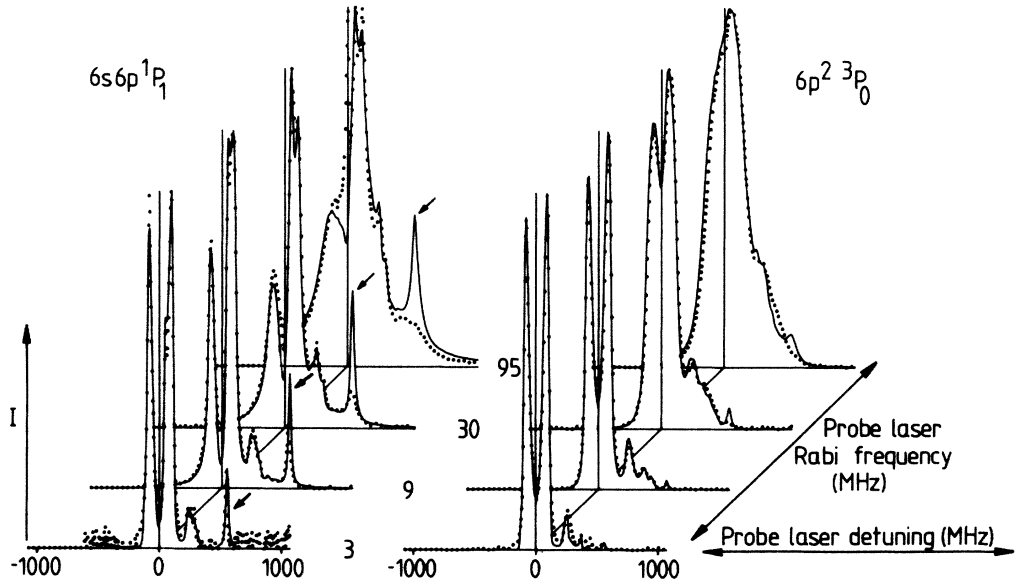

FIG. 7. Comparison of experimental profiles (dots) shown in Fig. 2 with theoretical profiles (solid lines). The strong laser was tuned to line center, and the strong-laser Rabi frequency was 200 MHz. The five most abundant isotopes of barium were included in the theoretical model. The arrows indicate the peaks due to the $F=\frac{1}{2}$ hyperfine component of the $6s\,6p\ ^1P_1$ levels of ^{137}Ba and ^{135}Ba.

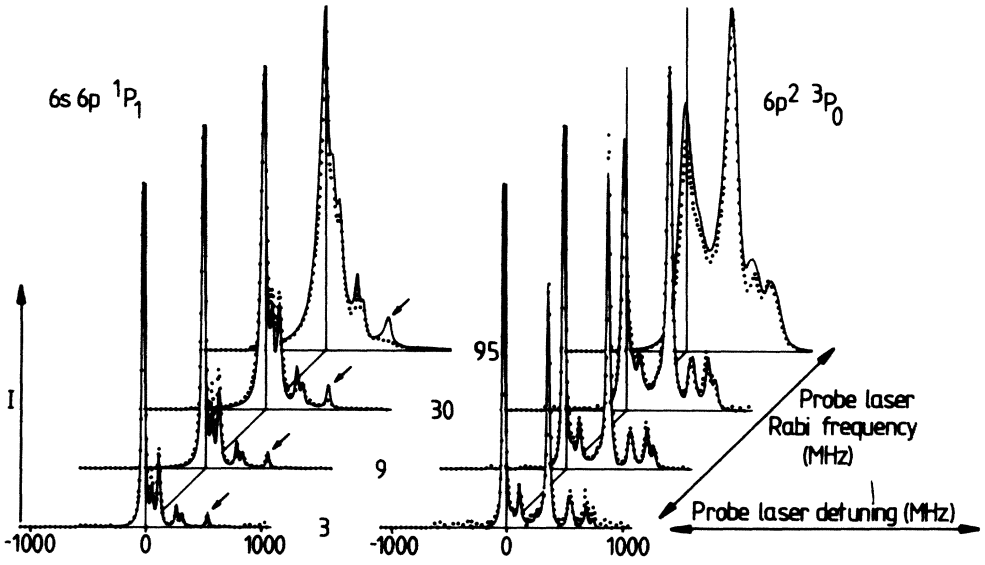

FIG. 8. Comparison of experimental profiles (dots) shown in Fig. 3 with theoretical profiles (solid lines). The strong laser was detuned -400 MHz from line center, and the strong-laser Rabi frequency was 200 MHz. The five most abundant isotopes of barium were included in the theoretical model. The arrows indicate the peaks due to the $F=\frac{1}{2}$ hyperfine component of the $6s\,6p\ ^1P_1$ levels of ^{137}Ba and ^{135}Ba.

since in this case the loss from the $M_F=\frac{1}{2}$ subsystem will be partially compensated by cross relaxation from the $M_F=\frac{3}{2}$ subsystem, and vice versa. The degree of this compensation will be a complicated function of the intensities and detunings of the two lasers, so the above correction to the $F=\frac{1}{2}$ hyperfine component was not applied in order to illustrate the possible magnitude of the errors which may be introduced by treating the two Zeeman subsystems separately. However, for reasons which will be explained later, the resolution of the present experiment was not sufficient to associate unambiguously any other deviations of the experimental profiles from the theoretical profiles with this approximation.

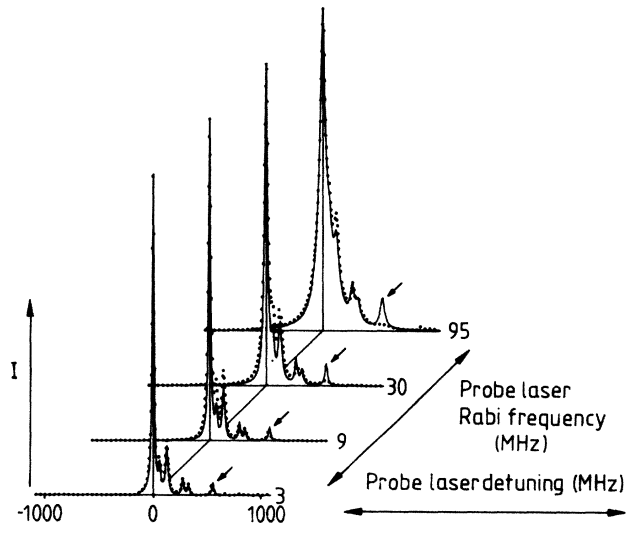

FIG. 9. Comparison of experimental profiles (dots) of the $6s\,6p\ ^1P_1$ level, obtained with the strong laser blocked, with theoretical profiles (solid lines). The five most abundant isotopes of barium were included in the theoretical model.

A series of experimental profiles obtained over a wide range of strong-laser detunings is compared with theoretical profile in Fig. 10. Due to computer time restrictions, the theoretical profiles for this comparison were calculated for ^{138}Ba only, resulting in discrepancies in regions where the fluorescence due to the less abundant isotopes is dominant. Nevertheless, these comparisons demonstrate that the development of the experimental profiles as the strong laser is detuned is at least in general agreement with theoretical predictions.

Due to the lack of a well-defined Autler-Townes doublet at zero strong-laser detuning for large probe-laser Rabi frequencies, the method[5] for superimposing the two laser waists at the interaction region was not usable. It was not possible to use neutral density filters to reduce the probe-laser Rabi frequency temporarily for this alignment, since the filters themselves produced a shift in the probe-laser waist position. As a result the estimated uncertainty in the superposition of the two beams was approximately ± 50 μm. This uncertainty was probably primarily responsible for the generally reduced agreement between the theoretical and experimental profiles for large probe-laser Rabi frequencies, compared with that for the case of the weak probe laser.[5] This conclusion was supported by the fact that it was possible to improve the agreement for the strong-probe case by introducing offsets, which varied from one experimental run to the next, between the axes of the two laser beams in the theoretical model.

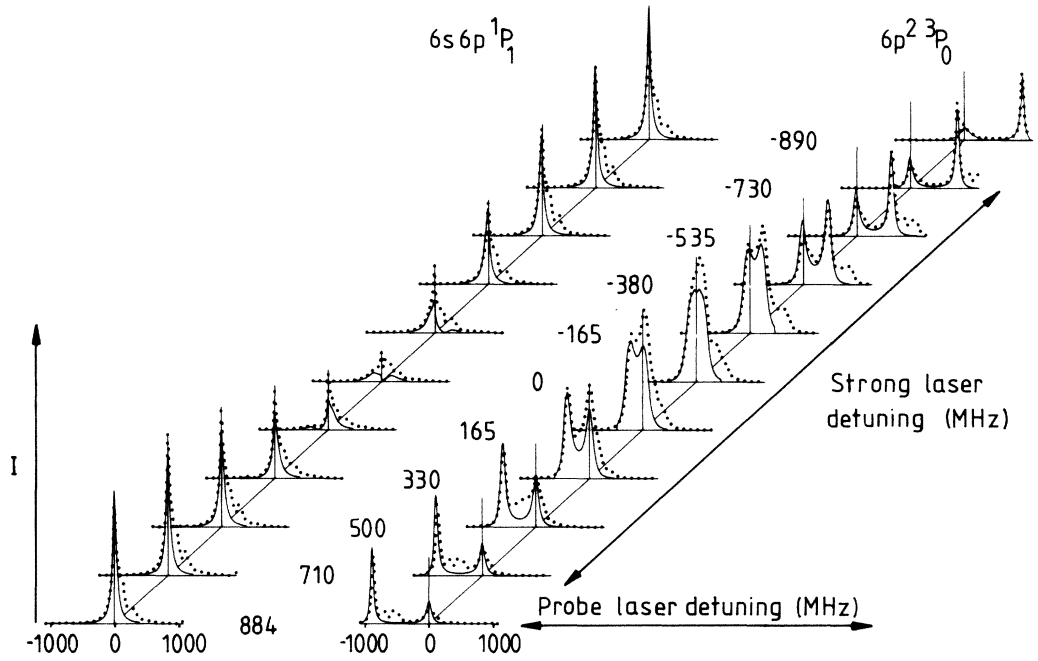

FIG. 10. Comparison between theoretical (solid lines) and experimental (dots) profiles obtained with strong- and probe-laser Rabi frequencies of 200 and 95 MHz, respectively. Only ^{138}Ba was included in the theoretical model.

VI. CONCLUSION

In conclusion, despite the inherent limitations on the precision of the experimental alignment, the comparison between theory and experiment presented in this paper has convincingly demonstrated that a theoretical model based on the Bloch equations can predict the results of this experiment throughout the range of laser intensities and detunings investigated.

In the strong-probe case it was found that when the 608.3-nm laser was detuned from exact resonance by an amount greater than the Rabi frequency of the interaction between the light from either laser and the 3LS, the population of the uppermost ($6p^2\,^3P_0$) level of the 3LS in ^{138}Ba was always maximized by detuning the 553.5 nm from exact resonance by the same amount in the opposite direction (i.e., to the two-photon resonance defined in Sec. III). This is in direct contrast to the corresponding situation in the weak-probe case in ^{138}Ba,[5] where the population of the uppermost level of the 3LS was maximized by tuning the 553.5-nm laser close to exact resonance.

The generality of the above result for the strong-probe case (i.e., two saturating laser radiation fields) was tested by varying the natural widths of the middle and upper levels of the 3LS in the theoretical model, and it was found that the same behavior is predicted even when the lifetime of the uppermost level was assumed to be longer than that of the middle level.

[1]J. L. Picque and J. Pinard, J. Phys. B **9**, L77 (1976).
[2]J. E. Bjorkholm and P. F. Liao, Opt. Commun. **21**, 132 (1977).
[3]H. R. Gray and C. R. Stroud, Opt. Commun. **25**, 359 (1978).
[4]C. Delsart, J. C. Keller, and V. P. Kaftandjian, J. Phys. (Paris) **42**, 529 (1981).
[5]P. T. H. Fisk, H.-A. Bachor, and R. J. Sandeman, Phys. Rev. A **33**, 2418 (1986).
[6]P. T. H. Fisk, H.-A. Bachor, and R. J. Sandeman, Phys. Rev. A **33**, 2424 (1986).
[7]For clarity and consistency with previous work, we shall continue to refer to this laser as the probe laser, although it is now permitted to affect the ground-state population substantially.
[8]L. Jahreiss and M. C. E. Huber, Phys. Rev. A **31**, 692 (1985).
[9]F. M. Kelly and M. S. Mathur, Can. J. Phys. **55**, 83 (1977).
[10]P. Hannaford and R. M. Lowe, Aust. J. Phys. (to be published).
[11]P. M. Radmore and P. L. Knight, J. Phys. B **15**, 561 (1982).
[12]H. R. Gray, R. M. Whitley, and C. R. Stroud, Opt. Lett. **3**, 218 (1978).
[13]R. M. Whitley and C. R. Stroud, Phys. Rev. A **14**, 1498 (1976).
[14]P. T. H. Fisk, Ph.D. thesis, Australian National University, (unpublished).
[15]M. C. E. Huber and S. Niggli (private communication).
[16]G. Nowicki, K. Bekk, S. Göring, A. Hanser, H. Rebel, and G. Schatz, Phys. Rev. C **18**, 2369 (1978).
[17]W. Jitschin and G. Meisel, Z. Phys. A **295**, 37 (1980).